LANGMUIR
Article
Cite This: Langmuir 2018, 34, 7210−7221
pubs.acs.org/Langmuir

Equilibrium Contact Angle and Adsorption Layer Properties with Surfactants

Uwe Thiele,*[,†,‡,§] Jacco H. Snoeijer,[∥] Sarah Trinschek,[†,⊥] and Karin John[⊥]

[†]Institut für Theoretische Physik, [‡]Center of Nonlinear Science (CeNoS), and [§]Center for Multiscale Theory and Computation (CMTC), Westfälische Wilhelms-Universität Münster, 48149 Münster, Germany

[∥]Physics of Fluids Group and J. M. Burgers Centre for Fluid Dynamics, University of Twente, P.O. Box 217, 7500 AE Enschede, The Netherlands

[⊥]Université Grenoble-Alpes, CNRS, Laboratoire Interdisciplinaire de Physique, 38000 Grenoble, France

ABSTRACT: The three-phase contact line of a droplet on a smooth surface can be characterized by the Young equation. It relates the interfacial energies to the macroscopic contact angle θ_e. On the mesoscale, wettability is modeled by a film-height-dependent wetting energy $f(h)$. Macro- and mesoscale descriptions are consistent if $\gamma \cos \theta_e = \gamma + f(h_a)$, where γ and h_a are the liquid−gas interface energy and the thickness of the equilibrium liquid adsorption layer, respectively. Here, we derive a similar consistency condition for the case of a liquid covered by an insoluble surfactant. At equilibrium, the surfactant is spatially inhomogeneously distributed, implying a nontrivial dependence of θ_e on surfactant concentration. We derive macroscopic and mesoscopic descriptions of a contact line at equilibrium and show that they are consistent only if a particular dependence of the wetting energy on the surfactant concentration is imposed. This is illustrated by a simple example of dilute surfactants, for which we show excellent agreement between theory and time-dependent numerical simulations.

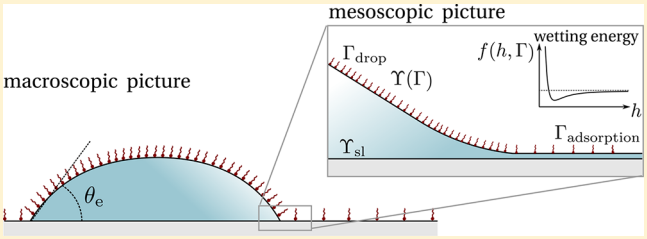

INTRODUCTION

Surfactants are amphiphilic molecules or particles that adsorb at interfaces, thereby decreasing the surface tension of the interface. Their chemicophysical properties crucially alter the dynamics of thin liquid films with free surfaces, a fact that is exploited for many industrial and biomedical applications, such as coating, deposition, and drying processes on surfaces and surfactant replacement therapy for premature infants. (See refs 1 and 2 for reviews.) However, the detailed mechanism of surfactant-driven flow is still an active field of research, experimentally and theoretically. In the simplest case, the spreading of surfactant-laden droplets on solid surfaces, the presence of surfactants leads to deviations from Tanner's law, namely, the spreading rate is $R(t) \propto t^{(1/4)}$ instead of $R(t) \propto t^{(1/10)}$ as expected for the pure liquid. (See ref 2 for a review.) The basic explanation of this phenomenon is that gradients in the surface tension are associated with interfacial (Marangoni) stresses which drive the fluid flow and the convective and diffusive transport of surfactant molecules along the interface. The surfactant concentration and the interfacial tension are related by an equation of state.

Besides the modified Tanner law, the interplay between surfactant dynamics and free-surface thin-film flow leads to a variety of intriguing phenomena, such as surfactant-induced fingering of spreading droplets,[2,2−7] superspreading of aqueous droplets on hydrophobic surfaces,[8,9] and autophobing of aqueous drops on hydrophilic substrates.[10−12] In addition to creating Marangoni stresses at the free interface, several other properties of surfactants enrich the spectrum of dynamical behaviors observed. Bulk solubility, their propensity to form micelles or lamellar structures at high concentrations, the surfactant mobility on the solid surface, and their ability to spread through the three-phase contact region are all key parameters influencing the flow properties. But the presence of surfactants does not only affect the flow dynamics. In the static situation of a surfactant-covered droplet on a substrate in equilibrium, the spatially inhomogeneous distribution of surfactant will also cause a nontrivial dependence of the contact angle on the surfactant concentration.

The governing equations that describe film flows and surfactant dynamics at low surfactant concentrations and in situations where the influence of wettability is negligible are well-established (See refs 13 and 14 for a review.) Typically, the dynamics of the liquid with a free surface is described using an evolution equation for the film height (derived from the lubrication approximation of viscous Stokes flow with a no-slip boundary condition at the substrate) coupled to an evolution equation of the surfactant concentration. The equations usually include capillarity (with a constant surface tension, though) and Marangoni stresses via an equation of state for the surfactant. Some models include wettability via a disjoining pressure in a mesoscopic approach[11,15,16] or model the influence of

Received: February 14, 2018
Revised: April 12, 2018
Published: May 14, 2018

DOI: 10.1021/acs.langmuir.8b00513
Langmuir 2018, 34, 7210−7221

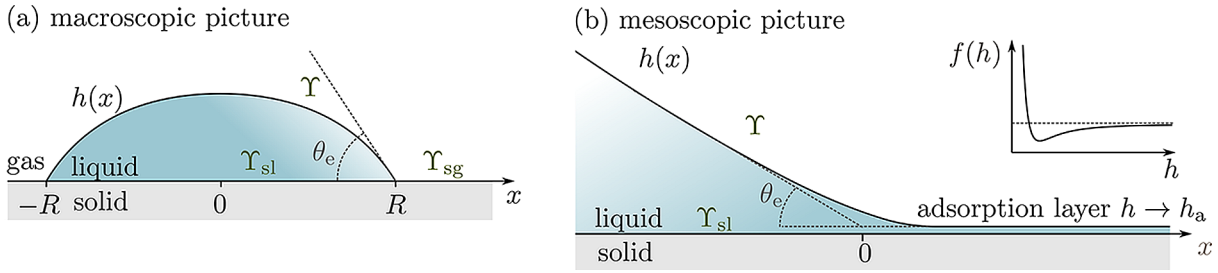

Figure 1. Liquid drop at a solid−gas interface. (a) In the macroscopic picture, the equilibrium contact angle θ_e is determined by the interfacial tensions Υ, Υ_{sl}, and Υ_{sg}, characterizing the liquid−gas, solid−liquid, and solid−gas interfaces, respectively. (b) In the mesoscopic picture, the substrate is covered by an equilibrium adsorption layer of height h_a which corresponds to the minimum in the wetting energy $f(h)$.

surfactants on the contact angle to obtain the contact line velocity in a macroscopic picture.[17] However, they do not discuss the consistency condition presented here. Often specific model features, e.g., nonlinear equations of state, are included at the level of the dynamic equations in an ad hoc fashion, thereby neglecting the fact that the passive-surfactant thin-film system has to respect symmetries imposed by the laws of thermodynamics. (See ref 13 for a review.)

The recent formulation of the dynamic equations in terms of thermodynamically consistent gradient dynamics[13,14] sheds some light on a more rigorous approach to modeling surfactant-driven thin-film flows using an energy functional. Following the approach from refs 13 and 14, we find that features such as nonlinear equations of state for the surfactant and concentration-dependent wettability can be included in a consistent manner in a mesoscopic description. However, what still needs to be established is the consistency of the mesoscopic approach with macroscopic parameters, i.e., the equilibrium contact angle of a droplet in the presence of surfactants. For droplets of pure liquids on a solid substrate, this relation is well known (refs 18−23 and references therein) and can be obtained by relating the mesoscopic parameters of the wetting energy to the macroscopic Young equation. A derivation can be found in ref 24, and the approach is discussed in ref 25 for different wetting scenarios.

Here we establish this mesoscopic−macroscopic link for the extended system: a droplet of a pure liquid in contact with a solid substrate covered by a liquid adsorption layer in the presence of insoluble surfactants. Our approach is based on a mesoscopic energy functional depending on the film height and the surfactant coverage profiles. We reveal the selection of the contact angle θ_e in the presence of surfactants. This involves a nontrivial coupling with the equilibration of surfactant concentrations, respectively, on the drop and on the liquid adsorption layer. These considerations are relevant for cases involving bare substrates or ultrathin films, where apolar and/or polar forces between interfaces become non-negligible and where the dynamics is governed by the contact line. For example, it has been proposed that the onset of Marangoni flow for surfactant-driven spreading and fingering of droplets on hydrophilic surfaces depends on the ability of the surfactant to diffuse in front of the droplet to establish a gradient, which then drives the flow.[6,7] Similarly, autophobing is associated with a transfer of surfactant onto the substrate to render it less hydrophilic,[10,11] leading to dewetting and film rupture. Although surfactant-induced flows are dynamic phenomena out of equilibrium, the underlying theoretical framework of linear flux−force relations has to be consistent with the equilibrium conditions at the meso- and macroscales.

The article is structured as follows. First, we revise how to derive the macroscopic and mesoscopic equilibrium descriptions for a surfactant-free droplet of a pure liquid on a solid substrate. This parallel approach establishes the link between the macroscopic variables (surfaces tensions) and the additional mesoscopic variables (wetting energy) via the Young law. While this part mainly reviews well-established considerations,[18−23] it serves as an introduction of our methodology that is subsequently applied in the next section in our consideration of drops covered by insoluble surfactants. We rely here strictly on the existence of a (generalized) Hamiltonian, which includes capillarity and a wetting energy that are both dependent on the surfactant concentration. No other assumptions about the underlying hydrodynamics of the problem are made. We show the conditions for consistency between the macroscopic and mesoscopic approaches in terms of the equilibrium contact angle and the equilibrium distribution of surfactants. Finally, we illustrate our calculations by explicitly choosing a functional form for the Hamiltonian, consistent with a linear equation of state for the surfactant, and we propose a simple modification of the disjoining pressure which yields consistency with the Young law in the presence of surfactants.

A DROP OF SIMPLE LIQUID (NO SURFACTANTS)

Macroscopic Consideration. We start by reviewing the derivation of the Laplace law and the Young law from a free-energy approach (compare the discussions in refs 19, 21, and 22) that we will later expand by incorporating surfactants. Let us consider a 2D liquid drop of finite volume, i.e., a cross section of a transversally invariant liquid ridge, that has contact lines at $x = \pm R$. (See the sketch in Figure 1a.) The liquid−gas, solid−liquid, and solid−gas free energy per area here directly correspond to the interface tensions and are denoted by Υ, Υ_{sl}, and Υ_{sg}, respectively. Using the drop's reflection symmetry, we write the (half) free energy as

$$\mathcal{F} = \int_0^R \mathrm{d}x\, [\Upsilon\xi + \Upsilon_{sl} - Ph] + \int_R^\infty \mathrm{d}x\, \Upsilon_{sg} + \lambda_h h(R) \tag{1}$$

where the metric factor is

$$\xi = (1 + (\partial_x h)^2)^{1/2} \tag{2}$$

and ∂_x denotes the derivative with respect to x. For small interface slopes, one can make the small-gradient or long-wave approximation

$$\xi \approx 1 + (\partial_x h)^2/2 \tag{3}$$

often used in gradient dynamics models on the interface Hamiltonian (a.k.a. thin-film or lubrication models).[26−28] The

DOI: 10.1021/acs.langmuir.8b00513
Langmuir 2018, 34, 7210−7221

liquid volume $V = \int \mathrm{d}x\ h$ is controlled via the Lagrange multiplier P.

We independently vary the profile $h(x)$ and the position of the contact line R. The two are coupled due to $h(R) = 0$, which is imposed through the Lagrange multiplier λ_h. Varying $h(x)$ implies

$$\delta\mathcal{F} = \left[\Upsilon\frac{\partial_x h}{\xi} + \lambda_h\right]\delta h(R) - \int_0^R \mathrm{d}x\ \delta h(x)\left[\Upsilon\frac{\partial_{xx}h}{\xi^3} + P\right] \tag{4}$$

which gives

$$\lambda_h = -\Upsilon\frac{\partial_x h}{\xi} \text{ for } x = R \tag{5}$$

$$P = -\Upsilon\kappa \text{ for } x \in [0, R] \tag{6}$$

where we introduced the curvature

$$\kappa = \frac{\partial_{xx}h}{\xi^3} \tag{7}$$

The variation of R evaluated at $x = R$ gives

$$\delta\mathcal{F} = [\Upsilon\xi + \Upsilon_{sl} - \Upsilon_{sg} - Ph + \lambda_h\partial_x h]\delta R \tag{8}$$

which together with the constraint $h(R) = 0$ and λ_h given by eq 5 results in the Young law

$$\Upsilon\cos\theta_e = \Upsilon_{sg} - \Upsilon_{sl} \tag{9}$$

where we employed

$$1/\xi = (1 + (\partial_x h(R))^2)^{-1/2} = \cos\theta_e \tag{10}$$

Note that a similar approach is also presented in refs 29 and 30, where a transversality condition at the boundary is used instead of a Lagrange multiplier that fixes $h(R) = 0$. Next, we remind the reader how to obtain the same law from considerations on the mesoscale.

Mesoscopic Consideration. We continue by reviewing the derivation of the mesoscopic relations from a free-energy approach (compare the discussions in refs 18−23) that will also later be expanded by incorporating surfactants. The starting point is an interface Hamiltonian derived from microscopic considerations, asymptotically or numerically (refs 31−34),

$$\mathcal{F} = \int_0^\infty \mathrm{d}x[\Upsilon\xi + \Upsilon_{sl} + f(h) - Ph] \tag{11}$$

with the same metric factor as defined in eq 2. As in eq 1, we consider only the half energy of a reflection-symmetric droplet. Here, $f(h)$ is the wetting potential[31,32] as depicted in Figure 1b. For partially wetting liquids, $f(h)$ normally has a minimum at some $h = h_a$ corresponding to the height of an equilibrium adsorption layer (in hydrodynamics often referred to as a "precursor film") and approaches zero as $h \to \infty$. Mathematically, $\mathcal{F}$ is a Lyapunov functional, thermodynamically it may be seen as a grand potential, and in a classical mechanical equivalent it would be an action (i.e., the integral over the Lagrangian, with position x and film height h playing the roles of time and position in classical point mechanics).

Now we vary $\mathcal{F}$ with respect to $h(x)$ and obtain

$$\delta\mathcal{F} = \int_0^\infty \mathrm{d}x\ \delta h(x)[-\Upsilon\kappa + \partial_h f - P] \tag{12}$$

where we used $[\Upsilon\frac{\partial_x h}{\xi}\delta h(x)]_0^\infty = 0$. On the basis of eq 12, the free surface profile is given by the Euler−Lagrange equation

$$0 = -\Upsilon\kappa + \partial_h f - P \tag{13}$$

i.e., the Laplace-Derjaguin equation in ref 23. Multiplying by $\partial_x h$ and integrating with respect to x gives the first integral. (Note that if the integrand in eq 11 is seen as Lagrangian L, then the generalized coordinate and corresponding momentum are $q = h$ and $p = \partial L/\partial(\partial_x h) = \Upsilon(\partial_x h)/\xi$, respectively. Then the first integral E corresponds to the negative of the Hamiltonian $H = p\partial_x q - L$.)

$$E = -\Upsilon\int\frac{\partial_x h}{\xi^3}\partial_{xx}h\ \mathrm{d}x + f(h) - Ph + \Upsilon_{sl} = \frac{\Upsilon}{\xi} + f(h) - Ph + \Upsilon_{sl} \tag{14}$$

where E is a constant that is independent of x. This first integral can be interpreted as an energy density or as the horizontal force acting on a cross-section of the film. The fact that E is constant reflects the horizontal force balance.

Now we consider the wedge geometry in Figure 1b and determine the thickness h_a of the coexisting adsorption layer on the right and the angle θ_e formed by the wedge on the left. To do so, we first consider eqs 13 and 14 in the wedge region far away from the adsorption layer, i.e., where the film height is sufficiently large that f, $\partial_h f \to 0$ and $hP \to 0$. Note that the mesoscopic wedge region with $\partial_x h \approx$ const is distinct from the region of the macroscopic droplet governed by the Laplace law $P = -\Upsilon\kappa$. (For a more extensive argument, see ref 24.)

This gives

$$P = 0 \tag{15}$$

$$E = \frac{\Upsilon}{\xi_w} + \Upsilon_{sl} \tag{16}$$

for the wedge. Second, we consider the adsorption layer far away from the wedge. There, eqs 13 and 14 result in

$$P = \partial_h f|_{h_a} \tag{17}$$

$$E = \Upsilon + f(h_a) - h_a P + \Upsilon_{sl} \tag{18}$$

Equilibrium states are characterized by a pressure P and a first integral E that are constant across the system. Therefore, the adsorption layer height h_a and the contact angle θ_e are given by

$$P = \partial_h f|_{h_a} = 0 \text{ and} \tag{19}$$

$$\frac{\Upsilon}{\xi_w} = \Upsilon\cos\theta_e = \Upsilon + f(h_a) \tag{20}$$

respectively.

Consistency between Mesoscopic and Macroscopic Approaches. Comparing eq 20 with the macroscopic Young law (eq 9) yields the expected relation

$$f(h_a) = \Upsilon_{sg} - \Upsilon_{sl} - \Upsilon = S \tag{21}$$

as a condition for the consistency between mesoscopic and macroscopic descriptions. S denotes the spreading coefficient. For small contact angles $\theta_e \ll 1$, eq 20 reads $f(h_a) = -\Upsilon\theta_e^2/2$.

We can now reinterpret the free energy in eq 11. The solid substrate with an adsorption layer corresponds to the "dry" region in the macroscopic free energy (eq 1). For consistency

DOI: 10.1021/acs.langmuir.8b00513
Langmuir 2018, 34, 7210−7221

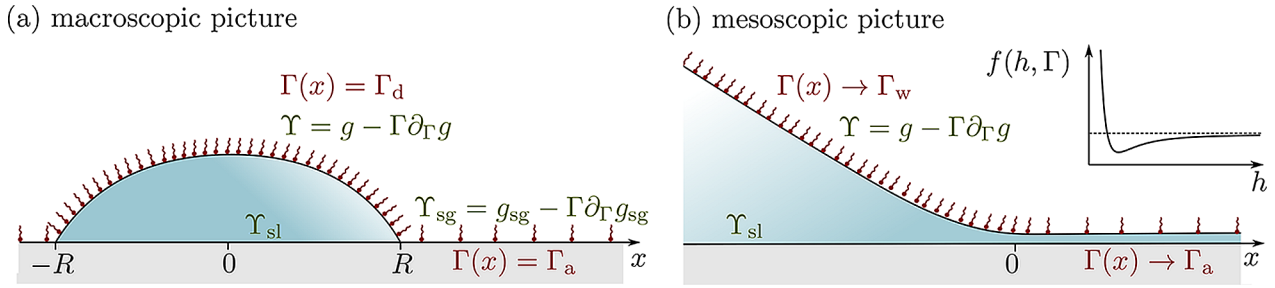

Figure 2. Liquid drop covered by insoluble surfactant at a solid−gas interface. (a) In the macroscopic approach, the equilibrium contact angle is determined by the solid−liquid interfacial tension Υ_{sl} and the liquid−gas and solid-gas interfacial tensions Υ and Υ_{sd} that depend on the respective surfactant concentrations Γ_d and Γ_a on the droplet and the adsorption layer. (b) In the mesoscopic picture, the substrate is covered by an equilibrium adsorption layer and the contact angle is determined by the liquid−gas interfacial tension Υ which depends on the surfactant concentration, the solid−liquid interfacial tension Υ_{sl}, and the minimum in the wetting energy $f(h_a)$.

at the energy level, the mesoscopic energy density should approach Υ_{sg} in the adsorption layer at $P = 0$; consequently, $f(h_a) = \Upsilon_{sg} - \Upsilon_{sl} - \Upsilon$, which leads also to eq 21. The solid substrate with an adsorption layer corresponds to the moist case in ref 19, where the energy density should approach Υ_{sg} (strictly speaking, Υ_{sg}^{moist}); consequently, $f(h_a) = \Upsilon_{sg}^{moist} - \Upsilon_{sl} - \Upsilon$ as for a flat equilibrium adsorption layer at $P = 0$. This implies that the moist spreading coefficient is $S^{moist} = f(h_a)$ which is well-defined as long as $f(h)$ has a minimum. Note that for $h \to 0$, in many approximations the wetting energy $f(h)$ shows an unphysical divergence. This may be avoided by employing a cutoff (see refs 19 and 29) or by determining $f(h)$ from proper microscopic models[33−36]. In the latter case, one finds a finite $f(0) = \Upsilon_{sg}^{dry} - \Upsilon_{sl} - \Upsilon = S^{dry}$ that is well-defined even for $f(h)$ without a minimum.

As an aside, we note that the calculation presented here is not exactly equivalent to the determination of a binodal for a binary mixture where the coexistence of two homogeneous phases is characterized by equal chemical potential and equal local grand potential. Here, the coexistence of a homogeneous phase (adsorption layer) and an inhomogeneous phase (wedge) is characterized by equal pressure P (corresponding to the chemical potential in the case of a binary mixture) and equal Hamiltonian E (which differs from the local grand potential, i.e., the integrand in eq 11, by a factor of $1/\xi^2$ in the liquid−gas interface term).

A LIQUID DROP COVERED BY INSOLUBLE SURFACTANTS

Macroscopic Consideration. We now consider insoluble surfactants, which exhibit a number density Γ (per unit area) on the free liquid−gas interface $h(x)$ (Figure 2a). There may also be surfactant at the solid−gas interface. The total amount of surfactant, $N = \int ds\, \Gamma = \int dx\, \xi\Gamma$, is conserved, which is imposed by a Lagrange multiplier λ_Γ. The liquid volume $V = \int dx\, h$ and the condition $h(R) = 0$ for a contact line at R are ensured via Lagrange multipliers P and λ_h, respectively. The surface free energies of the liquid−gas and solid−gas interfaces are characterized by functions $g(\Gamma)$ and $g_{sg}(\Gamma)$, respectively. The solid−liquid interface is first assumed to be free of surfactant.

As for the case of pure liquid, we first consider a macroscopic formulation in which the interaction of the liquid−gas interface (and surfactants) with the solid near the three-phase contact line is not made explicit. This is done in the mesoscopic model presented below.

The energy now to be minimized corresponds to a grand potential and reads

$$\mathcal{F}[h, \Gamma] = \int_0^R dx\, [\xi g(\Gamma) + \Upsilon_{sl} - Ph] + \int_R^\infty dx\, g_{sg}(\Gamma) - \lambda_\Gamma\left(\int_0^R dx\, \xi\Gamma + \int_R^\infty dx\, \Gamma\right) + \lambda_h h(R) \tag{22}$$

Varying the field $\Gamma(x)$ gives

$$\delta\mathcal{F} = \int_0^R dx\, \xi(\partial_\Gamma g - \lambda_\Gamma)\delta\Gamma + \int_R^\infty dx\, (\partial_\Gamma g_{sg} - \lambda_\Gamma)\delta\Gamma \tag{23}$$

resulting in

$$\lambda_\Gamma = \partial_\Gamma g \text{ for } x \in [0, R] \text{ and } \lambda_\Gamma = \partial_\Gamma g_{sg} \text{ for } x \in [R, \infty] \tag{24}$$

Since, in general, $\partial_\Gamma g$ is a function of Γ and λ_Γ is a constant, eq 24 implies that the surfactant is homogeneously distributed in each region, i.e.,

$$\partial_x\Gamma = 0 \tag{25}$$

We introduce equilibrium concentrations $\Gamma(x) = \Gamma_d$ on the droplet and $\Gamma(x) = \Gamma_a$ on the substrate. For the equilibrium distribution of surfactants with constant chemical potential λ_Γ, eq 24 reduces to

$$\partial_\Gamma g|_{\Gamma_d} = \partial_\Gamma g_{sg}|_{\Gamma_a} \tag{26}$$

Varying the field $h(x)$ gives

$$\begin{aligned}\delta\mathcal{F} &= \int_0^R dx \left[- P - \frac{\partial_{xx}h}{\xi^3}(g - \lambda_\Gamma\Gamma)\right]\delta h(x) \\ &\quad + \left[\left(\frac{\partial_x h}{\xi}(g - \lambda_\Gamma\Gamma)\right)\delta h\right]_0^R + \lambda_h\delta h(R) \\ &= \int_0^R dx\, [- P - \kappa\Upsilon]\delta h(x) + \left[\frac{\partial_x h}{\xi}\Upsilon + \lambda_h\right]\lambda_h(R)\end{aligned} \tag{27}$$

where we employed eq 24 and introduced the surfactant-dependent liquid−gas interface tension (a.k.a. the local grand potential or the mechanical tension in the interface or surface stress)

$$\Upsilon = g - \Gamma\partial_\Gamma g \tag{28}$$

Note that indeed for insoluble surfactants a Wilhelmy plate in a Langmuir trough measures Υ and not g as the area is changed at

DOI: 10.1021/acs.langmuir.8b00513
Langmuir 2018, 34, 7210−7221

a fixed amount of surfactant; i.e., Γ changes with the area. At the left boundary at $x = 0$, the reflection symmetry of the droplet enforces $\partial_x h = 0$. Equation 27 implies that the Laplace pressure and λ_h become

$$P = -\Upsilon\kappa \text{ for } x \in [0, R] \tag{29}$$

$$\lambda_h = -\Upsilon\frac{\partial_x h}{\xi} \text{ at } x = R \tag{30}$$

Finally, the variation of R evaluated at $x = R$ gives

$$\delta\mathcal{F} = [\xi g(\Gamma) + \Upsilon_{sl} - Ph - g_{sg}(\Gamma_a) - \lambda_\Gamma\xi\Gamma_d - \lambda_\Gamma\Gamma_a + \lambda_h\partial_x h(R)]\delta R \tag{31}$$

Using the constraint $h(R) = 0$ as well as the obtained values for λ_Γ and λ_h, this gives the boundary condition (using $1/\xi = \cos\theta_e$):

$$0 = \Upsilon_{sl} - \Upsilon_{sg}(\Gamma_a) + \Upsilon(\Gamma_d)\cos\theta_e \tag{32}$$

$$\text{with } \Upsilon(\Gamma_d) = g(\Gamma_d) - \Gamma_d\partial_\Gamma g|_{\Gamma_d} \tag{33}$$

$$\text{and } \Upsilon_{sg}(\Gamma_a) = g_{sg}(\Gamma_a) - \Gamma_a\partial_\Gamma g_{sg}|_{\Gamma_a} \tag{34}$$

In other words, we have again found the Young law that relates the interfacial tensions to the equilibrium contact angle. However, the interface tensions Υ_i do not correspond to the local free energies g and g_{sg} (which would enter at fixed concentration Γ) but rather on the local grand potentials $g - \Gamma\partial_\Gamma g$ and $g_{sg} - \Gamma\ \partial_\Gamma g_{sg}$ (valid at constant total amount of surfactant).

Importantly, the values of Υ and Υ_{sg} are not fixed a priori but have to be determined self-consistently from the equilibration of surfactant concentration, as given by eq 26. As such, the observed contact angle involves a subtle coupling between the mechanics and distribution of surfactants.

Mesoscopic Consideration. By analogy with the previous calculations for simple liquids where we developed mesoscopic considerations in the case without surfactant, we next discuss how to describe the case of insoluble surfactants on the mesoscale. Again, we focus on equilibrium situations involving a contact line (Figure 2b). Now it needs to be discussed how the dependency of the wetting potential on surfactant concentration has to be related to the respective dependencies of the involved surface energies to ensure consistency between mesoscopic and macroscopic descriptions.

A general discussion of a gradient dynamics description for the dynamics of liquid layers or drops covered by insoluble or soluble surfactants can be found in refs 13 and 14, respectively. There, various thermodynamically consistent extensions of thin film hydrodynamics without surfactants toward situations with surfactants are discussed and contrasted with literature approaches. Such extensions are, for instance, surfactant-dependent interface energies and wetting potentials that affect not only hydrodynamic flows but also diffusive fluxes. However, the intrinsic relations between wetting energy f and interface energy g were not discussed.

To begin with, we consider a general wetting energy $f(h, \Gamma)$ and interface energy $g(\Gamma)$. The resulting grand potential is

$$\mathcal{F}[h, \Gamma] = \int_0^\infty [\Upsilon_{sl} + f(h, \Gamma) + g(\Gamma)\xi - Ph - \lambda_\Gamma\Gamma\xi]\,dx \tag{35}$$

with ξ being again the metric factor (eq 2). P and λ_Γ are the Lagrange multipliers for the conservation of the amounts of liquid and surfactant, respectively. Note that first we treat the solid–liquid interface energy Υ_{sl} as constant.

Varying $h(x)$ and $\Gamma(x)$, we obtain from eq 35 the Euler–Lagrange equations

$$P = \partial_h f - \partial_x\left[(g - \lambda_\Gamma\Gamma)\frac{\partial_x h}{\xi}\right] \tag{36}$$

$$\text{and } \lambda_\Gamma = \frac{1}{\xi}\partial_\Gamma f + \partial_\Gamma g \tag{37}$$

respectively; i.e., the pressure P and chemical potential λ_Γ are constant across the system.

We use the mechanical approach introduced below eq 13 and introduce the generalized positions $q_1 = h$ and $q_2 = \Gamma$ and obtain from the local grand potential (integrand in eq 35, i.e., the Lagrangian) the generalized momenta $p_1 = (g - \lambda_\Gamma\Gamma)(\partial_x h)/\xi$ and $p_2 = 0$, respectively. Consequently, the first integral E is

$$E = \Upsilon_{sl} + f + \frac{g - \Gamma\lambda_\Gamma}{\xi} - hP \tag{38}$$

i.e., eq 14 with Υ replaced by $g(\Gamma) - \Gamma\lambda_\Gamma$. All equilibrium states are characterized by P, λ_Γ, and E, which are constant across the system. This allows us to investigate the coexistence of states.

As in the previously studied case of a drop without surfactants, we consider the equilibrium between a wedge region with constant slope $\tan\theta_e$ and an adsorption layer of thickness h_a (Figure 2b). As the wetting potential $f(h, \Gamma)$ depends on the film height and surfactant concentration, one needs to determine not only the coexisting wedge slope and adsorption layer height as in the case without surfactants but also the coexisting surfactant concentrations on the wedge, Γ_w, and on the adsorption layer, Γ_a. The considered wedge is far away from the adsorption layer ($h \gg h_a$, $f \to 0$, $|\partial_x h| \to \tan\theta_e$, $\Gamma \to \Gamma_w$), and the adsorption layer is far away from the wedge ($h \to h_a$, $\partial_x h \to 0$, $\Gamma \to \Gamma_a$); i.e., both are sufficiently far away from the contact line region. By comparing P, λ_Γ, and E from eqs 36, 37, and 38 in wedge and adsorption layer (by analogy with the calculation for the simple liquid), one finds

$$0 = \partial_h f|_{(h_a,\Gamma_a)} \tag{39}$$

$$\partial_\Gamma g|_{\Gamma_w} = \partial_\Gamma f|_{(h_a,\Gamma_a)} + \partial_\Gamma g|_{\Gamma_a} \tag{40}$$

$$\Upsilon(\Gamma_w)\cos\theta_e = f(h_a, \Gamma_a) - \Gamma_a\partial_\Gamma f|_{(h_a,\Gamma_a)} + \Upsilon(\Gamma_a) \tag{41}$$

respectively. To obtain eq 41, we have already used eqs 39 and 40 as well as $\xi_w = 1/\cos\theta_e$ and eq 28. Without surfactant, we recover eq 20 as $g(0)$ is Υ in the calculation for simple liquids.

The obtained eqs 39–41 allow one to determine the binodals for the wedge-adsorption layer coexistence. In practice, one may chose any of the four quantities θ_e, Γ_w, h_a, or Γ_a as control parameter and determine the other three from eqs 39–41. It is convenient to pick Γ_a as a control parameter and first use eq 39 to determine h_a and then employ eq 40 to obtain Γ_w and finally eq 41 to obtain the equilibrium contact angle θ_e. To obtain specific results, the wetting energy $f(h, \Gamma)$ and free energies of the liquid–gas interface $g(\Gamma)$ and the solid–gas interface $g_{sg}(\Gamma)$ have to be specified. A simple but illustrative example is discussed in the Application for Simple Energy section.

Consistency between Mesoscopic and Macroscopic Approaches. Equation 41 is the generalization of the

DOI: 10.1021/acs.langmuir.8b00513
Langmuir 2018, 34, 7210–7221

mesoscopic Young law (eq 20) for the treated case with surfactant. As the concentrations are different on the wedge ($\Gamma = \Gamma_w$) and on the adsorption layer ($\Gamma = \Gamma_a$), the liquid−gas interface tensions are also different. Equation 41 is accompanied by eqs 39 and 40, which provide the adsorption layer height and the relation between Γ_w and Γ_a, respectively. A comparison of the mesoscopic Young law (eq 41) with the macroscopic one (eq 34) implies

$$f(h_a, \Gamma_a) - \Gamma_a \partial_\Gamma f|_{(h_a,\Gamma_a)} = \Upsilon_{sg}(\Gamma_a) - \Upsilon_{sl} - \Upsilon(\Gamma_a) = S(\Gamma_a) \tag{42}$$

This corresponds to a generalization of the consistency condition (eq 21) for the case with surfactant. It relates the macroscopic equations of state (or interface energies) with the height- and surfactant-dependent wetting energy. (Note that alternatively one may, instead of eq 28, define $\Upsilon = g - \Gamma\partial_\Gamma g - \Gamma/\xi\partial_\Gamma f$, rendering eqs 14 and 20 formally valid at the cost of introducing a surfactant-, film height- and film slope-dependent surface tension.)

We have used the fact that the surfactant concentrations should be identical in the macroscopic and mesoscopic descriptions. Note that the surfactant concentration Γ_w on the wedge in the mesoscopic picture corresponds to the concentration Γ_d on the droplet in the macroscopic picture, as can be seen from eq 37. The consistency of the surfactant concentrations in both descriptions implies another condition, namely, that the macroscopic chemical equilibrium (eq 24) $\partial_\Gamma g|_{\Gamma_w} = \partial_\Gamma g_{sg}|_{\Gamma_a}$ has to coincide with the mesoscopic one (eq 40), i.e., $\partial_\Gamma g|_{\Gamma_w} = \partial_\Gamma f|_{(h_a,\Gamma_a)} + \partial_\Gamma g|_{\Gamma_a}$. Comparing the two conditions implies

$$\partial_\Gamma g_{sg}|_{\Gamma_a} = \partial_\Gamma f|_{(h_a,\Gamma_a)} + \partial_\Gamma g|_{\Gamma_a} \tag{43}$$

Introducing the resulting relation for $\partial_\Gamma f|_{(h_a,\Gamma_a)}$ into eq 42 results in

$$f(h_a, \Gamma_a) = g_{sg}(\Gamma_a) - \Upsilon_{sl} - g(\Gamma_a) \tag{44}$$

In the next section, we explore the consequences of the consistency conditions for a relatively simple case. First, we assume a low surfactant concentration resulting in purely entropic interfacial energies $g(\Gamma)$ and $g_{sg}(\Gamma)$ before extending the result to arbitrary g.

APPLICATION FOR SIMPLE ENERGY

In the next section, we illustrate our examples for a simple free energy which describes the situation of a low concentration of surfactant. We employ a wetting energy that is a product of height- and concentration-dependent factors, i.e., the presence of surfactant changes only the contact angle but not the adsorption layer height.

Macroscopic Consideration. We consider a low-concentration insoluble surfactant (similar to an ideal gas) on the solid−gas and the liquid−gas interfaces. In general, even in the dilute limit, the surfactant will affect the liquid−gas and solid−gas interfaces differently; i.e., the relevant molecular scales a will differ due to different effective molecular areas. Thus, we write the surface free energies $g(\Gamma)$ and $g_{sg}(\Gamma)$ as

$$g(\Gamma) = \Upsilon^0 + \frac{k_B T}{a^2}\Gamma(\ln\Gamma - 1) \tag{45}$$

$$g_{sg}(\Gamma) = \Upsilon^0_{sg} + \frac{k_B T}{a^2_{sg}}\Gamma(\ln\Gamma - 1) \tag{46}$$

respectively; i.e., we introduce different effective molecular length scales a and a_{sg}. This results in

$$\Upsilon(\Gamma) = g - \Gamma\partial_\Gamma g = \Upsilon^0 - \frac{k_B T}{a^2}\Gamma \tag{47}$$

$$\Upsilon_{sg}(\Gamma) = g_{sg} - \Gamma\partial_\Gamma g_{sg} = \Upsilon^0_{sg} - \frac{k_B T}{a^2_{sg}}\Gamma \tag{48}$$

in which the purely entropic free energy results in a linear equation of state. The macroscopic concentration-dependent $\Upsilon_{sg}(\Gamma_a)$ reflects the fact that the solid−gas interface is moist as it is covered by the adsorption layer, and at equilibrium, surfactant is found on the drop as well as on the adsorption layer. As a result, the solid−gas interface tension Υ_{sg} in the macroscopic picture aggregates the effects of surfactant on wetting energy *and* interface energy Υ.

By inserting these interface energies into the modified Young law (eq 34), we find

$$\cos\theta_e = \frac{\cos\theta_{e0} - \epsilon_1\delta\Gamma_a}{1 - \epsilon_1\Gamma_d} \tag{49}$$

with θ_{e0} being the contact angle in the absence of surfactant, $\delta = \frac{a^2}{a^2_{sg}}$ being the ratio of the different molecular length scales, and $\epsilon_1 = k_B T/(a^2\Upsilon^0)$ being a positive constant. The ratio of surfactant concentrations follows directly from eq 26 as

$$\Gamma_d = \Gamma_a^{a^2/a^2_{sg}} = \Gamma_a^\delta \tag{50}$$

We discuss a number of limiting cases which distinguish between different ratios of the molecular length scales.

(A) The dependencies of the interface energies g and g_{sg} on surfactant are identical, i.e., $a = a_{sg}$ and therefore $\delta = a^2/a^2_{sg} = 1$. The surfactant concentrations on the adsorption layer and drop are identical ($\Gamma_d = \Gamma_a = \Gamma$). The observable dependence of the equilibrium contact angle θ_e on the surfactant concentration takes the form

$$\cos\theta_e = \frac{\cos\theta_{e0} - \epsilon_1\Gamma}{1 - \epsilon_1\Gamma} \tag{51}$$

in which the contact angle would monotonically increase with the surfactant concentration, giving rise to the effect of autophobing.

(B) The surfactant prefers to stay on the liquid−gas interface, i.e., $a \ll a_{sg}$ and $\delta = a^2/a^2_{sg} \ll 1$. This implies $\Gamma_d \gg \Gamma_a$. The equilibrium contact angle shows the following functional dependence on the surfactant concentration:

$$\cos\theta_e \approx \frac{\cos\theta_{e0}}{1 - \epsilon_1\Gamma_d} \tag{52}$$

This case corresponds to the classical surfactant effect, which decreases the equilibrium contact angle with increasing concentration.

(C) The surfactant prefers to stay on the solid−gas interface, i.e., $a \gg a_{sg}$ and $\delta = a^2/a^2_{sg} \gg 1$, which implies $\Gamma_d \ll \Gamma_a$. The equilibrium contact angle shows the following functional dependence on the surfactant concentration:

$$\cos\theta_e \approx \cos\theta_{e0} - \epsilon_1\delta\Gamma_d \tag{53}$$

DOI: 10.1021/acs.langmuir.8b00513
Langmuir 2018, 34, 7210−7221

This case corresponds to a strong autophobing effect, which increases the equilibrium contact angle with increasing surfactant concentration. These limiting cases illustrate that the dependency of θ_e on the amount of surfactant depends subtly on the nature of the free energies. Below, this will be further investigated numerically.

Mesoscopic Consideration. We again consider a low-concentration insoluble surfactant (similar to an ideal gas) on the liquid−gas interface with the ideal gas local free energy $g(\Gamma)$ as defined in eq 45 and the liquid−gas interface tension $\Upsilon(\Gamma)$ as defined in eq 47. Note that g_{sg} does not occur in the mesoscopic description as the whole domain is at least covered by an adsorption layer. Furthermore, we use the strong assumption that the wetting energy may be factored as

$$f(h, \Gamma) = \chi(\Gamma)\hat{f}(h) \tag{54}$$

with $\chi(0) = 1$. This allows us to investigate the case of a surfactant that influences the contact angle but does not change the adsorption layer height. The surfactant-independent adsorption layer height h_a is still given by $\partial_h \hat{f}|_{h_a} = P$ as in the case of the simple liquid. The equilibrium contact angle θ_e is obtained by inserting the product ansatz (eq 54) for $f(h, \Gamma)$ into eq 41, which results in

$$\Upsilon(\Gamma_w)\cos\theta_e = \Upsilon(\Gamma_a) + \hat{f}(h_a)[\chi(\Gamma_a) - \Gamma_a \partial_\Gamma \chi|_{\Gamma_a}] \tag{55}$$

Note that the restriction to a simple product ansatz implies that one is not able to investigate surfactant-induced wetting transitions characterized by a diverging adsorption layer height, and we expect the ansatz to break down for $\theta_e \to 0$. This will be further discussed elsewhere. (In general, it is known[22] that two (independent) critical exponents characterize the change in wetting behavior close to the wetting transition. They characterize (i) how $\cos(\theta_e) \to 1$ and (ii) how the thickness of the adsorption layer diverges. Choosing a product ansatz corresponds to the limiting case of a zero critical exponent for the adsorption layer height.)

Consistency between Mesoscopic and Macroscopic Approaches. The concentration dependence of $\chi(\Gamma)$ in eq 54 can not be chosen freely but needs to account for the consistency condition between the mesoscopic and macroscopic picture. By inserting the product ansatz (eq 54) for the wetting energy and the entropic local free energies into eq 44, which ensures the consistency between the two approaches, we obtain

$$\chi(\Gamma_a) = 1 = M\Gamma_a(\ln(\Gamma_a - 1)) \text{ with } M = \frac{k_B T}{\hat{f}(h_a)}\left(\frac{1}{a^2} - \frac{1}{a_{sg}^2}\right) \tag{56}$$

As this expression has to hold for any Γ_a, the wetting energy can be written as

$$f(h, \Gamma) = \hat{f}(h)\left[1 - \frac{k_B T}{\hat{f}(h_a)}\left(\frac{1}{a^2} - \frac{1}{a_{sg}^2}\right)\Gamma(\ln\Gamma - 1)\right] \tag{57}$$

Let us summarize the mesoscopic and macroscopic approaches for a drop covered by insoluble surfactant. Macroscopically, the situation is completely determined by g, g_{sg}, and Υ_{sl}. This allows for a given Γ_a or Γ_d to obtain the other Γ and the contact angle θ_e.

Mesoscopically, g_{sg} is not defined, but via the consistency conditions, it is reflected in the wetting energy $f(h, \Gamma)$ that itself is not part of the macroscopic description. In the special case treated in this section, g is determined by a, the macroscopic quantity g_{sg} is determined by a_{sg}, and the concentration dependence of the mesoscopic $f(h, \Gamma)$ depends on both a and a_{sg}.

Numerical Simulations for Surfactant-Covered Drops on a Finite Domain. To illustrate the equilibrium solutions of the model for finite domains, we perform numerical time simulations of the evolution equations for film height and surfactant concentration. The emerging equilibrium states which arise in the time simulations at large times are then compared to the analytical predictions. As discussed in refs 13 and 14, the evolution equations for a thin film covered by an insoluble surfactant can be written in the form of gradient dynamics of the mesoscopic free energy functional F given in eq 35 by introducing the projection of the surfactant concentration onto the flat surface of the substrate $\tilde{\Gamma} = \xi\Gamma$

$$\partial_t h = \nabla\cdot\left[Q_{hh}\nabla\frac{\delta F}{\delta h} + Q_{h\Gamma}\nabla\frac{\delta F}{\delta\tilde{\Gamma}}\right] \tag{58}$$

$$\partial_t \tilde{\Gamma} = \nabla\cdot\left[Q_{\Gamma h}\nabla\frac{\delta F}{\delta h} + Q_{\Gamma\Gamma}\nabla\frac{\delta F}{\delta\tilde{\Gamma}}\right] \tag{59}$$

where the respective mobilities are denoted as Q_{ij} and given by

$$\mathbf{Q} = \begin{pmatrix} Q_{hh} & Q_{\Gamma h} \\ Q_{h\Gamma} & Q_{\Gamma\Gamma} \end{pmatrix} = \begin{pmatrix} \frac{h^3}{3\eta} & \frac{h^2\Gamma}{2\eta} \\ \frac{h^2\Gamma}{2\eta} & \frac{h^2\Gamma}{\eta} + D\Gamma \end{pmatrix} \tag{60}$$

In the following, we consider the wetting energy

$$f(h, \Gamma) = \chi(\Gamma)\hat{f}(h) = \chi(\Gamma)\frac{A}{2h^2}\left(\frac{2h_a^3}{5h^3} - 1\right) \tag{61}$$

where $\hat{f}(h)$ consists of two power laws and for $A > 0$ describes a partially wetting fluid that macroscopically forms a droplet of finite contact angle on a stable adsorption layer of height h_a.

For the numerical analysis, the model is rescaled, introducing the length scale $l = h_a$. The solutions are characterized by three dimensionless parameters $\epsilon_1 = \frac{k_B T}{a^2\Upsilon^0}$, $\epsilon_2 = -\frac{10\hat{f}(h_a)}{3\Upsilon_0} = \frac{A}{h_a^2\Upsilon_0}$ and $\delta = \frac{a^2}{a_{sg}^2}$. These are connected to the ratio between the entropic contribution of the surfactant and the interfacial tension without surfactant, the equilibrium contact angle without surfactant, and the ratio of the effective molecular length scales of the surfactant at the liquid−gas and solid−gas interfaces, respectively.

Starting with a droplet on an adsorption layer covered by a homogeneous surfactant concentration $\Gamma(x) = \bar{\Gamma}$ as the initial condition, the evolution equations are solved using a finite element scheme provided by the DUNE-PDELAB modular toolbox.[37,38] The simulation domain $\Omega = [0, L_x]$ with $L_x/l = 200$ is discretized on an equidistant mesh of $N_x = 256$ quadratic elements with linear test and ansatz functions. No-flux boundary conditions are applied for both fields, corresponding to fixed amounts of fluid and surfactant in the system. For the time integration, we employ an implicit Runge−Kutta scheme with an adaptive time step and use the change in contact angle

DOI: 10.1021/acs.langmuir.8b00513
Langmuir 2018, 34, 7210−7221

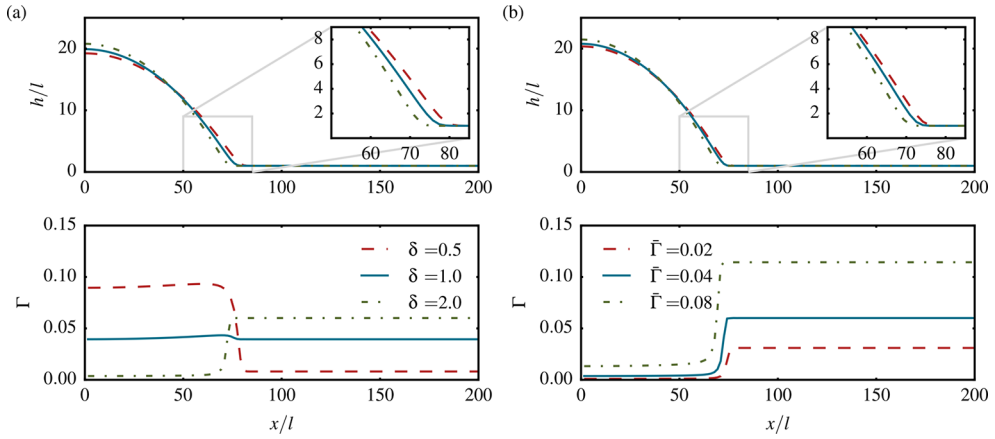

Figure 3. Profiles of film height h (top) and surfactant concentration Γ (bottom) evolving in the numerical simulations for large times. The simulations are performed for three different ratios $\delta = \frac{a^2}{a_{sg}^2}$ of the effective molecular length scales of the surfactant at $\bar{\Gamma} = 0.04$ in (a) and three different mean surfactant concentrations $\bar{\Gamma}$ at $\delta = 2$ in (b) while keeping the remaining parameters fixed at $\epsilon_1 = 0.2$ and $\epsilon_2 = 0.4$. The insets show a close-up view of the contact line region. Note that the surfactant concentration Γ_w which occurs on the wedge in the mesoscopic description corresponds to the concentration Γ_d on the droplet.

as the criterion to terminate the simulation when an equilibrium state is reached.

Figure 3 shows the profiles for film height and surfactant concentration to which the system converges for long times. As examples, we study three different ratios δ of the effective molecular length scales of the surfactant while keeping the remaining parameters fixed at $\epsilon_1 = 0.2$ and $\epsilon_2 = 0.4$. The resulting profiles deviate only slightly from a spherical cap shape in the contact line region and confirm the limiting cases (A−C) discussed in the macroscopic description of the system. If the dependencies of interface energies g and g_{sg} are identical, i.e., $a = a_{sg}$ and thus $\delta = 1$ (solid blue lines), then the surfactant concentration is identical on the drop and adsorption layer. The addition of surfactant to the system has in this case only a small effect on the contact angle. If the surfactant prefers to stay on the liquid−gas interface [$a < a_{sg}$ and thus $\delta < 1$ (dashed red lines)], then the surfactant accumulates on the droplet and the contact angle is slightly lowered. If the surfactant prefers to stay on the solid−gas interface [$a > a_{sg}$ and thus $\delta > 1$ (dashed−dotted green lines)], then the surfactant concentration on the drop is smaller than on the adsorption layer and the contact angle of the droplet increases. From the numerical time simulations, we extract the surfactant concentrations on the adsorption layer and on the droplet as well as the equilibrium contact angle and compare it to the analytically obtained equilibrium conditions (eqs 49 and 50) using the surfactant concentration on the adsorption layer Γ_a as a control parameter. In the time simulations, different amounts of surfactant are simply implemented by changing the initial concentration of surfactant $\bar{\Gamma}$. Figure 4 shows for three different values of δ the analytically obtained equilibrium values (eqs 49 and 50) depending on Γ_a as solid lines and the values extracted from time simulations with $L_x/l = 200$ (diamonds). The surfactant concentrations measured in the time simulation (top) match the analytical prediction very well. However, there is a small discrepancy in the contact angles (bottom). In order to understand this offset and test the hypothesis that it can be attributed to finite size effects, we analyze the steady state solutions using parameter continuation[39] employing the AUTO-07p software package.[40] The dashed lines in Figure 4 show the concentration Γ_w and $\cos(\theta_e)$ obtained by parameter

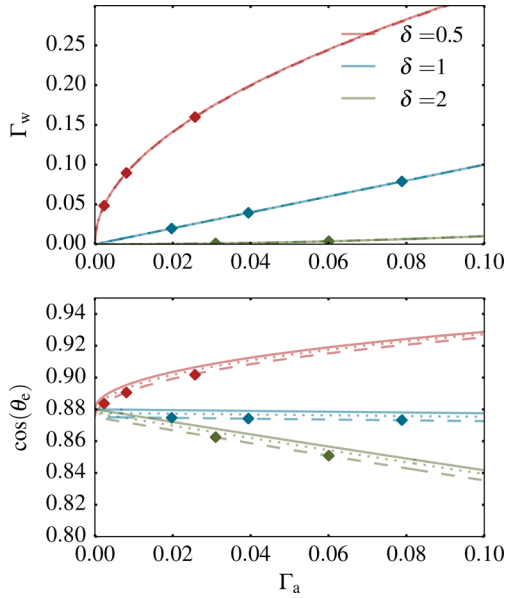

Figure 4. Surfactant concentration on the droplet (top) and equilibrium contact angle (bottom) depending on the surfactant concentration in the adsorption layer. The analytically obtained equilibrium conditions (solid lines) are compared to values extracted from time simulations (diamonds) for three values of δ. The dashed (dotted lines) show the values obtained by parameter continuation for domain size $L_x/l = 200$ ($L_x/l = 700$). The discrepancy in the equilibrium contact angle between the numerical and the analytical result can be attributed to finite size effects.

continuation for a domain and droplet size that correspond to the values used in the time simulations. If the domain size is increased to $L_x/l = 700$ with an accordingly adjusted liquid volume, then the values obtained by parameter continuation (dotted lines) are very close to the analytical prediction. The observed deviation of the time simulations can thus be explained by the finite size of the simulation domain and droplet. For very large domain and droplet sizes, the analytical predictions for surfactant concentration and contact angle match perfectly.

DOI: 10.1021/acs.langmuir.8b00513
Langmuir 2018, 34, 7210−7221

Generalization to Arbitrary Interface Energies. Having established the form of the function $\chi(\Gamma)$ which guarantees the consistency between the macroscopic and mesoscopic approaches for the equilibrium contact angle, we can now write a free energy on the mesoscale which is consistent with the macroscale. Identifying χ with

$$\chi = \frac{1}{\hat{f}_a}[g_{sg}(\Gamma) - g(\Gamma)] \tag{62}$$

we can rewrite eq 35 as

$$\mathcal{F}[h, \Gamma] = \int \left\{ \Upsilon_{sl} + \frac{\hat{f}(h)}{\hat{f}_a}[g_{sg}(\Gamma) - g(\Gamma)] + \xi[g(\Gamma) - \lambda\Gamma] - Ph \right\} dx \tag{63}$$

We now split the energy functional into three contributions stemming from the droplet $\mathcal{F}_{drop}$, the contact line region $\mathcal{F}_{int}$, and the adsorption layer $\mathcal{F}_a$, i.e., $\mathcal{F} = \mathcal{F}_{drop} + \mathcal{F}_{int} + \mathcal{F}_a$. In the droplet, away from the contact line, eq 63 simplifies to

$$\mathcal{F}_{drop} = \int \{\Upsilon_{sl} + \xi[g(\Gamma) - \lambda\Gamma] - Ph\}\, dx \tag{64}$$

whereas in the adsorption layer we find

$$\mathcal{F}_a = \int \{\Upsilon_{sl} + g_{sg} - \lambda\Gamma\}\, dx \tag{65}$$

where we have dropped the pressure term Ph_a in F_a by assuming that outside the adsorption layer $h \gg h_a$ and that the volume constraint on the liquid is determined by the droplet and not the adsorption layer. Expressions 64 and 65 are now identical to eq 22 in the macroscopic description of droplets covered by insoluble surfactants. This shows that the expression for $\chi(\Gamma)$ given in eq 62 is valid for all expressions g if the product ansatz for $f(h, \Gamma)$ is used.

Adsorption of Surfactant on the Substrate. A possible generalization of the model is to consider a surfactant which can accumulate at all three interfaces. The present section summarizes the basic results of this general case. We start with the macroscopic considerations, and to avoid confusion, we introduce the three different concentrations of surfactants Γ, Ω, and Σ at the liquid−gas, solid−liquid, and solid−gas interfaces, respectively. Then, the liquid−gas, solid−gas, and solid−liquid interfaces are characterized by surfactant-dependent local free energies $g(\Gamma)$, $g_{sg}(\Sigma)$, and $g_{sl}(\Omega)$, respectively. The energy to be minimized corresponds to the grand potential

$$\mathcal{F}[h, \Gamma, \Omega, \Sigma] = \int_0^R dx\, [\xi g(\Gamma) + g_{sl}(\Omega) - Ph] + \int_R^\infty dx\, g_{sg}(\Sigma) - \lambda_\Gamma\left(\int_0^R dx\, (\xi\Gamma + \Omega) + \int_R^\infty dx\, \Sigma\right) + \lambda_h h(R) \tag{66}$$

For a fixed overall amount of surfactant, one again obtains eqs 32−34 in generalized form

$$0 = \Upsilon_{sl}(\Omega) - \Upsilon_{sg}(\Sigma) + \Upsilon(\Gamma)\cos\theta_e \tag{67}$$

with

$$\Upsilon_{sl} = g_{sl}(\Omega_d) - \Omega_d \partial_\Omega g_{sl}|_{\Omega_d} \tag{68}$$

$$\Upsilon_{sg} = g_{sg}(\Sigma_a) - \Sigma_a \partial_\Sigma g_{sg}|_{\Sigma_a} \tag{69}$$

$$\Upsilon = g(\Gamma_d) - \Gamma_d \partial_\Gamma g|_{\Gamma_d} \tag{70}$$

The surfactant concentrations are related by $\partial_\Gamma g|_{\Gamma=\Gamma_d} = \partial_\Sigma g_{sg}|_{\Sigma=\Sigma_a} = \partial_\Omega g_{sl}|_{\Omega=\Omega_d}$; i.e., the chemical potential of surfactants is uniform across the entire system. The incorporation of surfactant also at the solid−liquid interface thus renders the discussion more involved but does not pose a principal problem.

Following the approach used in the mesoscopic description of droplets covered by insoluble surfactants, we include the adsorption of surfactants at the solid−liquid interface in the mesoscale considerations. However, in contrast to the macroscopic approach we consider only the surfactant concentrations at the liquid−gas and solid−liquid interfaces, Γ and Ω. The surfactant concentration in the adsorption layer in the mesoscopic description $\Gamma_a + \Omega_a$ is equivalent to the macroscopic solid−gas interface concentration $\Sigma_a = \Gamma_a + \Omega_a$. By analogy to eq 35, we write the grand potential

$$\mathcal{F}[h, \Gamma, \Omega] = \int_0^\infty [g_{sl}(\Omega) + f(h, \Gamma, \Omega) + g(\Gamma)\xi - Ph - \lambda_\Gamma(\Gamma\xi + \Omega)]\, dx \tag{71}$$

and obtain after variation with respect to h, Γ, and Ω the equilibrium conditions

$$0 = \partial_h f|_{(h_a, \Gamma_a, \Omega_a)} \tag{72}$$

$$\partial_\Gamma g|_{\Gamma_w} = \partial_\Gamma f|_{(h_a, \Gamma_a, \Omega_a)} + \partial_\Gamma g|_{\Gamma_a} \tag{73}$$

$$\partial_\Omega g_{sl}|_{\Omega_w} = \partial_\Omega f|_{(h_a, \Gamma_a, \Omega_a)} + \partial_\Omega g_{sl}|_{\Omega_a} \tag{74}$$

$$\partial_\Omega g\,|_{\Omega_w} = \partial_\Gamma g|_{\Gamma_w} \tag{75}$$

$$\Upsilon(\Gamma_w)\cos\theta_e + \Upsilon_{sl}(\Omega_w) = f(h_a, \Gamma_a, \Omega_a) - \Gamma_a \partial_\Gamma f|_{(h_a, \Gamma_a, \Omega_a)} - \Omega_a \partial_\Omega f|_{(h_a, \Gamma_a, \Omega_a)} + \Upsilon_{sl}(\Omega_a) + \Upsilon(\Gamma_a) \tag{76}$$

where subscripts "a" and "w" denote quantities on the adsorption layer side and the liquid wedge side, respectively. Equation 76 is the generalization of the mesoscopic Young law with surfactants on all three interfaces. Comparison with the macroscopic Young law (eq 67) implies the macro−meso consistency condition

$$f(h_a, \Gamma_a, \Omega_a) - \Gamma_a \partial_\Gamma f|_{(h_a, \Gamma_a, \Omega_a)} - \Omega_a \partial_\Omega f|_{(h_a, \Gamma_a, \Omega_a)} = \Upsilon_{sg}(\Sigma_a) - \Upsilon_{sl}(\Omega_a) - \Upsilon(\Gamma_a) \tag{77}$$

Equation 77 relates the macroscopic equations of state (or interface energies) with the height- and surfactant-dependent wetting energy. Furthermore, the condition that the macroscopic and mesoscopic chemical potentials of the surfactants coincide simplifies eq 77 to

$$f(h_a, \Gamma_a, \Omega_a) = g_{sg}(\Sigma_a) - g_{sl}(\Omega_a) - g(\Gamma_a) \tag{78}$$

The generalization of the product ansatz (eqs 62 and 63) immediately leads to a consistent form of the grand potential

DOI: 10.1021/acs.langmuir.8b00513
Langmuir 2018, 34, 7210−7221

$$\mathcal{F}[h, \Gamma, \Omega] = \int \left\{ \xi g(\Gamma) + g_{sl}(\Omega) - \lambda_\Gamma(\Omega + \xi\Gamma) + \frac{\hat{f}(h)}{\hat{f}_a}[g_{sg}(\Gamma + \Omega) - g(\Gamma) - g_{sl}(\Omega)] - Ph \right\} dx \tag{79}$$

with the equilibrium conditions for the surfactants being

$$\frac{\partial g_{sg}}{\partial \Omega}|_{\Omega_a,\Gamma_a} = \frac{\partial g_{sg}}{\partial \Gamma}|_{\Omega_a,\Gamma_a} = \frac{\partial g_{sl}}{\partial \Omega}|_{\Omega_w,\Gamma_w} = \frac{\partial g}{\partial \Gamma}|_{\Omega_w,\Gamma_w}$$
$$\text{with } \Gamma_a = \Omega_a \tag{80}$$

and the mesoscopic Young law being

$$\Upsilon(\Gamma_w)\cos\theta_e + \Upsilon_{sl}(\Omega_w) = \Upsilon_{sg}(\Gamma_a + \Omega_a) \tag{81}$$

CONCLUSIONS AND OUTLOOK

We have employed equilibrium considerations to establish the link between mesoscopic and macroscopic descriptions of drops covered by insoluble surfactants that rest on smooth, solid substrates. The requirement of consistency between the two approaches relates the macroscopic quantities (interface tensions) to the mesoscopic quantities (wetting energy) and implies that the dependencies of interface and wetting energies on surfactant concentration may not be chosen independently. In particular, the solid−gas interface tension in the macroscopic description is directly related to the properties of the mesoscopic wetting energy.

The main conclusions of our equilibrium results also apply to the theoretical description of out-of-equilibrium phenomena through hydrodynamic modeling. In particular, the surfactant dependencies of Derjaguin (or disjoining) pressures and interface tensions may not be chosen independently as this might result in (i) incorrect dynamics toward equilibrium and (ii) incorrect final states, i.e., those that do not correspond to minima of appropriate energy functionals. We emphasize that although many phenomena associated with surfactants, such as autophobing and spreading, are typically studied in dynamic and out-of-equilibrium settings, an underlying mesoscopic theoretical framework should at long times always lead to the same equilibrium state as the corresponding macroscopic description. Furthermore, we point out that the interpretation of experiments on surfactant-induced autophobing and other dynamical effects associated with surfactants would also benefit from an analysis of the corresponding equilibrium state as a basis for understanding the dynamic behavior.

If one does not take the consistency relation into account and chooses in the mesoscopic model the surfactant dependencies of liquid−gas interface tension and wetting energy without keeping the macroscopic system in mind, then one may implicitly assume quite peculiar surfactant dependencies of the solid−gas interface tension. (For instance, the linear dependencies of the Hamaker constant and liquid−gas interface tension on surfactant concentration employed in section V.C.1 of ref 15 imply a solid−gas interface tension of the form $c_1 + c_2\Gamma + c_3(1+\Gamma)^{n/(m-n)}$), where c_i represents constants and n and m are the powers in a polynomial wetting energy.)

In the Application for Simple Energy section, we have used a specific example to illustrate how the wetting energy (and Derjaguin pressure) needs to be modified in the presence of surfactants with a linear equation of state to ensure consistency between the macroscopic and mesoscopic pictures. Note that the employed ansatz of a factorized wetting energy $f(h) = \hat{f}(h)\chi(\Gamma)$ was chosen for simplicity. It is just one possible choice and actually strongly restricts the physical phenomena that can be described. To model the behavior close to a wetting transition, other assumptions regarding the form of the wetting energy need to be made as the product ansatz fixes the height of the adsorption layer while at a wetting transition it diverges.

The main arguments and results of our work are, however, of a general nature. They are independent of the exact form of the wetting energy. We find that in the presence of surfactant the structural form of the Young law remains unchanged, but the surfactant concentrations and surface tensions equilibrate self-consistently. Depending on the relation of the interface free energies of liquid−gas and solid−gas interfaces, adding surfactant may have qualitatively different effects on the contact angle. Even in our simple example with purely entropic surfactant free energies, we find either a lowering of the contact angle with increasing amount of surfactant in the system or the opposite behavior, i.e., autophobing. The approach proposed here together with the general dynamic models introduced in refs 13 and 14 allows for systematic numerical investigations of drop spreading and retraction dynamics employing mesoscopic models with consistent dependencies of wetting energy and interface tensions on surfactant concentration. For overviews of rich spreading, autophobing, and fingering behavior in various experiments, see refs 3 and 41−45,\.

As our approach is generic, it may be extended to a number of more complex situations. One example is a generalization toward soluble surfactants. Then, additionally a bulk concentrations of surfactants has to be incorporated under the static consideration. (For fully dynamic thin-film models, see ref 14.) The incorporation of micelles is also possible.

In principle, the local free energies (or equation of state) for the surfactant may be arbitrarily complicated and account for phase transitions of the surfactant. This can include substrate-induced phase transitions as substrate-mediated condensation.[46,47] If such transitions can occur, then the free energy also has to account for gradient contributions in the surfactant concentration. (See the extensions discussed in refs 13 and 14.) The approach developed here would then again give consistency relations between interface and wetting energies and include the possibility of phase changes in the surfactant layer.

In the current work, we have restricted ourselves to the analysis of equilibrium states. However, following the gradient dynamics ansatz of refs 13 and 14, our approach provides a basis to derive dynamic equations for the evolution of film height and surfactant concentrations, consistent with macroscopic models. The use of a wetting energy and the resultant Derjaguin (or disjoining) pressure formulation avoids, for example, ad hoc assumptions regarding a contact line law, a typical problem of macroscopic descriptions of the dynamics. The gradient dynamic approach building on the present static considerations can be applied to a variety of phenomena, for example, the dynamics of autophobing,[12] surfactant-induced dewetting,[48] and surfactant-assisted spreading and fingering instabilities.[3,7]

Finally, we point out that the presented approach can form a basis for consistent mesoscopic and macroscopic considerations regarding line tension and its influence on contact line stability in systems with surfactants as extensively studied for pure

DOI: 10.1021/acs.langmuir.8b00513
Langmuir 2018, 34, 7210−7221

liquids; see, for example, refs 18, 20, 49, and 50. As we have excluded line tension effects from our macroscopic Young law, our results are strictly speaking valid only for large droplets as discussed for pure liquids in ref 49. We expect that a consideration of these questions on the basis of the presented consistent mesoscopic and macroscopic approaches to systems with surfactants can result in an interesting discussion of coupled line tension and line surfactant concentration, i.e., a (positive or negative) excess surfactant concentration in the contact line region.

AUTHOR INFORMATION

Corresponding Author

*E-mail: u.thiele@uni-muenster.de.

ORCID

Sarah Trinschek: 0000-0003-1745-5784

Funding

We thank the DAAD, Studienstiftung des deutschen Volkes, Campus France (PHC PROCOPE grant 35488SJ) and the CNRS (grant PICS07343) for financial support. LIPhy is part of LabEx Tec 21 (Invest. l'Avenir, grant ANR-11-LABX-0030).

Notes

The authors declare no competing financial interest.

REFERENCES

(1) Craster, R.; Matar, O. Dynamics and stability of thin liquid films. *Rev. Mod. Phys.* **2009**, *81*, 1131.

(2) Matar, O.; Craster, R. Dynamics of surfactant-assisted spreading. *Soft Matter* **2009**, *5*, 3801−3809.

(3) Marmur, A.; Lelah, M. D. The spreading of aqueous surfactant solutions on glass. *Chem. Eng. Commun.* **1981**, *13*, 133−143.

(4) Troian, S.; Wu, X.; Safran, S. Fingering instability in thin wetting films. *Phys. Rev. Lett.* **1989**, *62*, 1496.

(5) Troian, S.; Herbolzheimer, E.; Safran, S. Model for the fingering instability of spreading surfactant drops. *Phys. Rev. Lett.* **1990**, *65*, 333.

(6) Cachile, M.; Cazabat, A.; Bardon, S.; Valignat, M.; Vandenbrouck, F. Spontaneous spreading of surfactant solutions on hydrophilic surfaces. *Colloids Surf., A* **1999**, *159*, 47−56.

(7) Cachile, M.; Cazabat, A. Spontaneous spreading of surfactant solutions on hydrophilic surfaces: C_n E_m in ethylene and diethylene glycol. *Langmuir* **1999**, *15*, 1515−1521.

(8) Hill, R. Superspreading. *Curr. Opin. Colloid Interface Sci.* **1998**, *3*, 247−254.

(9) Rafaï, S.; Sarker, D.; Bergeron, V.; Meunier, J.; Bonn, D. Superspreading: aqueous surfactant drops spreading on hydrophobic surfaces. *Langmuir* **2002**, *18*, 10486−10488.

(10) Afsar-Siddiqui, A.; Luckham, P.; Matar, O. Dewetting Behavior of Aqueous Cationic Surfactant Solutions on Liquid Films. *Langmuir* **2004**, *20*, 7575−7582.

(11) Craster, R.; Matar, O. On autophobing in surfactant-driven thin films. *Langmuir* **2007**, *23*, 2588−2601.

(12) Bera, B.; Duits, M.; Cohen Stuart, M.; van den Ende, D.; Mugele, F. Surfactant induced autophobing. *Soft Matter* **2016**, *12*, 4562−4571.

(13) Thiele, U.; Archer, A. J.; Plapp, M. Thermodynamically consistent description of the hydrodynamics of free surfaces covered by insoluble surfactants of high concentration. *Phys. Fluids* **2012**, *24*, 102107. Note that a term was missed in the variation of *F* and a correction is contained in the appendix of ref 14.

(14) Thiele, U.; Archer, A. J.; Pismen, L. M. Gradient dynamics models for liquid films with soluble surfactant. *Phys. Rev. Fluids* **2016**, *1*, 083903.

(15) Warner, M.; Craster, R.; Matar, O. Dewetting of ultrathin surfactant-covered films. *Phys. Fluids* **2002**, *14*, 4040−4054.

(16) Jensen, O.; Grotberg, J. Insoluble surfactant spreading on a thin viscous film: shock evolution and film rupture. *J. Fluid Mech.* **1992**, *240*, 259−288.

(17) Karapetsas, G.; Craster, R. V.; Matar, O. K. On surfactant-enhanced spreading and superspreading of liquid drops on solid surfaces. *J. Fluid Mech.* **2011**, *670*, 5−37.

(18) Churaev, N. V.; Starov, V. M.; Derjaguin, B. V. The shape of the transition zone between a thin-film and bulk liquid and the line tension. *J. Colloid Interface Sci.* **1982**, *89*, 16−24.

(19) de Gennes, P.-G. Wetting: Statics and dynamics. *Rev. Mod. Phys.* **1985**, *57*, 827−863.

(20) Dobbs, H.; Indekeu, J. Line tension at wetting - interface displacement model beyond the gradient-squared approximation. *Phys. A* **1993**, *201*, 457−481.

(21) de Gennes, P.-G.; Brochard-Wyart, F.; Quéré, D. *Capillarity and Wetting Phenomena: Drops, Bubbles, Pearls, Waves*; Springer: New York, 2004.

(22) Bonn, D.; Eggers, J.; Indekeu, J.; Meunier, J.; Rolley, E. Wetting and spreading. *Rev. Mod. Phys.* **2009**, *81*, 739−805.

(23) Starov, V. M.; Velarde, M. G. Surface forces and wetting phenomena. *J. Phys.: Condens. Matter* **2009**, *21*, 464121.

(24) Sharma, A. Equilibrium contact angles and film thicknesses in the apolar and polar systems: Role of intermolecular interactions in coexistence of drops with thin films. *Langmuir* **1993**, *9*, 3580−3586.

(25) Brochard-Wyart, F.; di Meglio, J.-M.; Quéré, D.; de Gennes, P.-G. Spreading of Nonvolatile Liquids in a Continuum Phase. *Langmuir* **1991**, *7*, 335−338.

(26) Oron, A.; Davis, S.; Bankoff, S. Long-scale evolution of thin liquid films. *Rev. Mod. Phys.* **1997**, *69*, 931−980.

(27) Thiele, U. Thin film evolution equations from (evaporating) dewetting liquid layers to epitaxial growth. *J. Phys.: Condens. Matter* **2010**, *22*, 084019.

(28) Yin, H.; Sibley, D.; Thiele, U.; Archer, A. Films, layers and droplets: The effect of near-wall fluid structure on spreading dynamics. *Phys. Rev. E: Stat. Phys., Plasmas, Fluids, Relat. Interdiscip. Top.* **2017**, *95*, 023104.

(29) Snoeijer, J. H.; Andreotti, B. A microscopic view on contact angle selection. *Phys. Fluids* **2008**, *20*, 057101.

(30) Bormashenko, E. Young, Boruvka-Neumann, Wenzel and Cassie-Baxter equations as the transversality conditions for the variational problem of wetting. *Colloids Surf., A* **2009**, *345*, 163−165.

(31) Dietrich, S. In *Wetting Phenomena*; Domb, C., Lebowitz, J. L., Eds.; Phase Transitions and Critical Phenomena; Academic Press: London, 1988; Vol. *12*; p 1.

(32) Schick, M. In *Introduction to Wetting Phenomena*; Charvolin, J., Joanny, J. F., Zinn-Justin, J., Eds.; Elsevier Science Publishers: North-Holland, 1990; p 415.

(33) Tretyakov, N.; Müller, M.; Todorova, D.; Thiele, U. Parameter passing between Molecular Dynamics and continuum models for droplets on solid substrates: The static case. *J. Chem. Phys.* **2013**, *138*, 064905.

(34) Hughes, A. P.; Thiele, U.; Archer, A. J. Influence of the fluid structure on the binding potential: Comparing liquid drop profiles from density functional theory with results from mesoscopic theory. *J. Chem. Phys.* **2017**, *146*, 064705.

(35) MacDowell, L. Computer simulation of interface potentials: Towards a first principle description of complex interfaces? *Eur. Phys. J.: Spec. Top.* **2011**, *197*, 131.

(36) Hughes, A. P.; Thiele, U.; Archer, A. J. Liquid drops on a surface: using density functional theory to calculate the binding potential and drop profiles and comparing with results from mesoscopic modelling. *J. Chem. Phys.* **2015**, *142*, 074702.

(37) Bastian, P.; Blatt, M.; Dedner, A.; Engwer, C.; Klöfkorn, R.; Kornhuber, R.; Ohlberger, M.; Sander, O. A generic grid interface for parallel and adaptive scientific computing. Part I: abstract framework. *Computing* **2008**, *82*, 103−119.

(38) Bastian, P.; Blatt, M.; Dedner, A.; Engwer, C.; Klöfkorn, R.; Kornhuber, R.; Ohlberger, M.; Sander, O. A generic grid interface for

DOI: 10.1021/acs.langmuir.8b00513
Langmuir 2018, 34, 7210−7221

parallel and adaptive scientific computing. Part II: Implementation and tests in DUNE. *Computing* **2008**, *82*, 121−138.
(39) Dijkstra, H. A.; Wubs, F. W.; Cliffe, A. K.; Doedel, E.; Dragomirescu, I. F.; Eckhardt, B.; Gelfgat, A. Y.; Hazel, A.; Lucarini, V.; Salinger, A. G.; Phipps, E. T.; Sanchez-Umbria, J.; Schuttelaars, H.; Tuckerman, L. S.; Thiele, U. Numerical Bifurcation Methods and their Application to Fluid Dynamics: Analysis beyond Simulation. *Commun. Comput. Phys.* **2014**, *15*, 1−45.
(40) Doedel, E. J.; Oldeman, B. E. *AUTO07p: Continuation and Bifurcation Software for Ordinary Differential Equations*; Concordia University: Montreal, 2009.
(41) Frank, B.; Garoff, S. Origins of the complex motion of advancing surfactant solutions. *Langmuir* **1995**, *11*, 87−93.
(42) Bardon, S.; Cachile, M.; Cazabat, A. M.; Fanton, X.; Valignat, M. P.; Villette, S. Structure and dynamics of liquid films on solid surfaces. *Faraday Discuss.* **1996**, *104*, 307−316.
(43) Stoebe, T.; Lin, Z.; Hill, R.; Ward, M.; Davis, H. Surfactant-enhanced spreading. *Langmuir* **1996**, *12*, 337−344.
(44) Starov, V. M.; Kosvintsev, S. R.; Velarde, M. G. Spreading of surfactant solutions over hydrophobic substrates. *J. Colloid Interface Sci.* **2000**, *227*, 185−190.
(45) Sharma, R.; Kalita, R.; Swanson, E.; Corcoran, T.; Garoff, S.; Przybycien, T.; Tilton, R. Autophobing on Liquid Subphases Driven by the Interfacial Transport of Amphiphilic Molecules. *Langmuir* **2012**, *28*, 15212−15221.
(46) Riegler, H.; Spratte, K. Structural-changes in lipid monolayers during the Langmuir-Blodgett transfer due to substrate monolayer interactions. *Thin Solid Films* **1992**, *210-211*, 9−12.
(47) Köpf, M. H.; Gurevich, S. V.; Friedrich, R.; Thiele, U. Substrate-mediated pattern formation in monolayer transfer: a reduced model. *New J. Phys.* **2012**, *14*, 023016.
(48) Qu, D.; Suter, R.; Garoff, S. Surfactant self-assemblies controlling spontaneous dewetting. *Langmuir* **2002**, *18*, 1649−1654.
(49) Widom, B. Line tension and the shape of a sessile drop. *J. Phys. Chem.* **1995**, *99*, 2803−2806.
(50) Brinkmann, M.; Kierfeld, J.; Lipowsky, R. Stability of liquid channels or filaments in the presence of line tension. *J. Phys.: Condens. Matter* **2005**, *17*, 2349−2364.

DOI: 10.1021/acs.langmuir.8b00513
Langmuir 2018, 34, 7210−7221